Detector Design and Analysis Technique for Local Electric Field Fluctuation Diagnostic Using Spatial Heterodyne Spectroscopy

Galen Burke

R.J. Fonck, G. Mckee, G.R. Winz

APS DPP, Portland

November 9, 2018

Introduction

Understanding Turbulence in Tokamaks is a Fundamental Challenge for Fusion Energy

- Plasma turbulence in tokamaks results in anomalous transport
  - Cross-field transport ≫ neoclassical predictions
- Present plasma diagnostics measure key fluctuating parameters $\tilde{n}$, $\tilde{T}_i$, $\tilde{T}_e$, $\tilde{v}$
- Measurement of electrostatic field turbulence ($\tilde{E} \sim k_\perp \tilde{\phi}$) remains a challenge, gives $\tilde{v}$
  - $\tilde{E}_\theta \times B_\phi \cong \tilde{v}_r$: turbulent cross-field transport, $\tilde{E}_r \times B_\phi \cong \tilde{v}_\theta$: shear-flow and zonal flow dynamics
- Local magnetic field fluctuation ($\tilde{B}$) measurement also challenging, could provide critical information
  - 3D magnetic field perturbation penetration into plasma pedestal

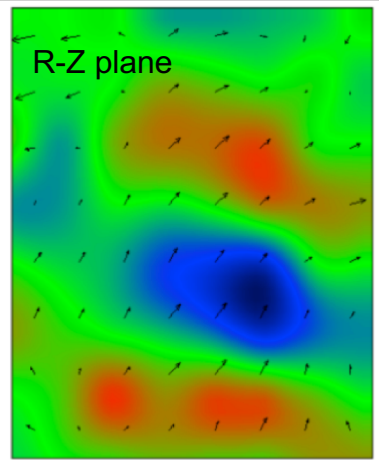

Density perturbations and calculated velocimetry in DIII-D plasma

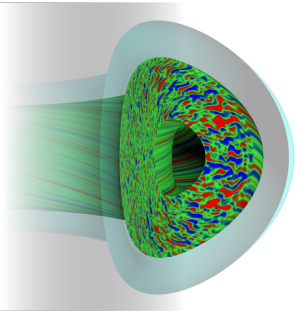

GYRO turbulence simulation

Motional Stark Effect Field Used as Carrier Signal for $\tilde{E}$

- Local plasma fluctuations → Stark multiplet fluctuations

$$\mathbf{E_t} = \mathbf{v}_b \times \mathbf{B} + \mathbf{E_p} + \mathbf{v}_b \times \tilde{\mathbf{B}} + \tilde{\mathbf{E}}_\mathbf{p}$$

$$\tilde{\Delta}_{Stark} \propto \tilde{\mathbf{E}}_\mathbf{t}$$

- Measure high-speed variations in π/σ line intensity ratio or in π-components line separation to derive $\tilde{E}$ or $\tilde{B}$
- Spatial Heterodyne Spectrometer (SHS) provides high throughput analyzer of multiplet spectrum
- New CMOS imaging system provide detection and DAQ

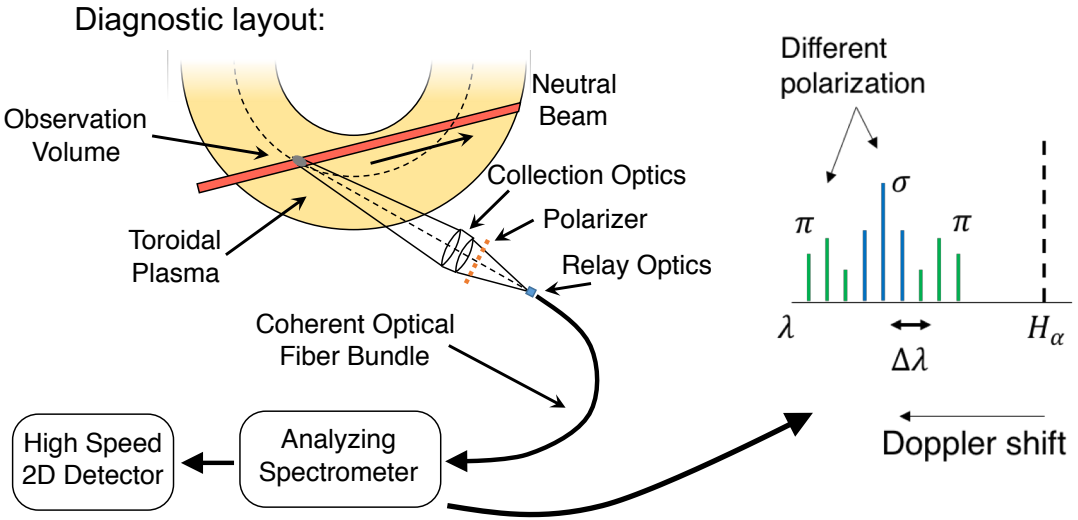

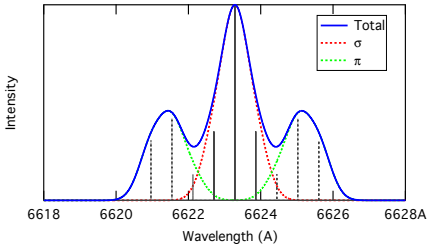

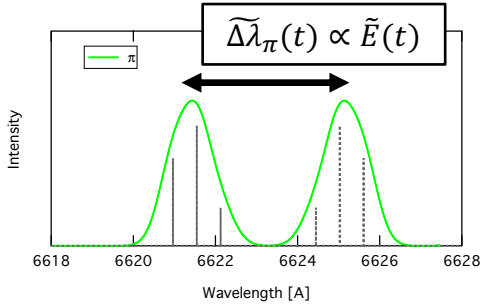

Model Hα Stark Spectrum: 80 keV, 0.5 T

$\tilde{E}/\vec{E}_{MSE}$ in Fusion Grade Plasmas ~10^{-3}

Experiment	$T_{e,0}$ (keV)	B (T)	a (m)	$\tilde{E}/E_{MSE}$
NSTX-U	~2-4	1	0.6	$1-2\times10^{-3}$
DIII-D	2-5	2	0.7	$0.5-1\times10^{-3}$
Pegasus	~0.3	0.3	0.35	$0.7-1\times10^{-3}$

- Tokamak drift wave turbulence scaling gives $\tilde{E} \propto T_e/a$
- $\tilde{E}$ turbulence broadband, majority of fluctuation power < 300 kHz
- $\tilde{E}$, $\tilde{n}$ rise from core to edge
- $\tilde{E}/E_{MSE}$ at or bellow photon noise floor for BES (typical rms noise ~1%)
  - Two independent but spatially correlated measurements (e.g. $\langle \tilde{E}\tilde{n} \rangle$) made simultaneously can suppress incoherent photon noise another ~10x

Fluctuations in TEXT

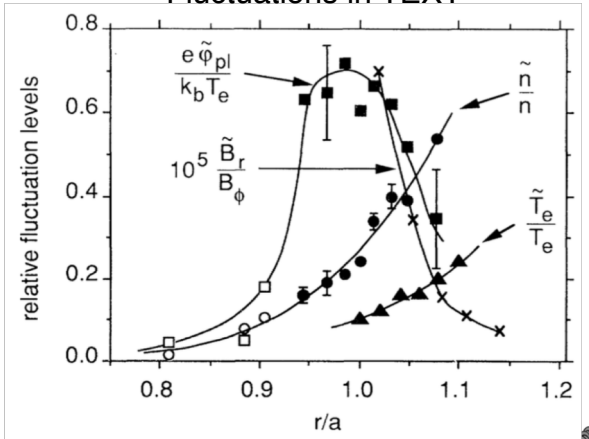

C. P. Ritz, et. al., Phys. Rev. Lett., **62**, 1989.

Spatial Heterodyne Spectroscopy Technique Utilized for $\Delta\tilde{\lambda}_\pi(t)$ Measurement

- Self scanned, 2 beam interferometer
- Input wavelengths heterodyned around Littrow wavelength

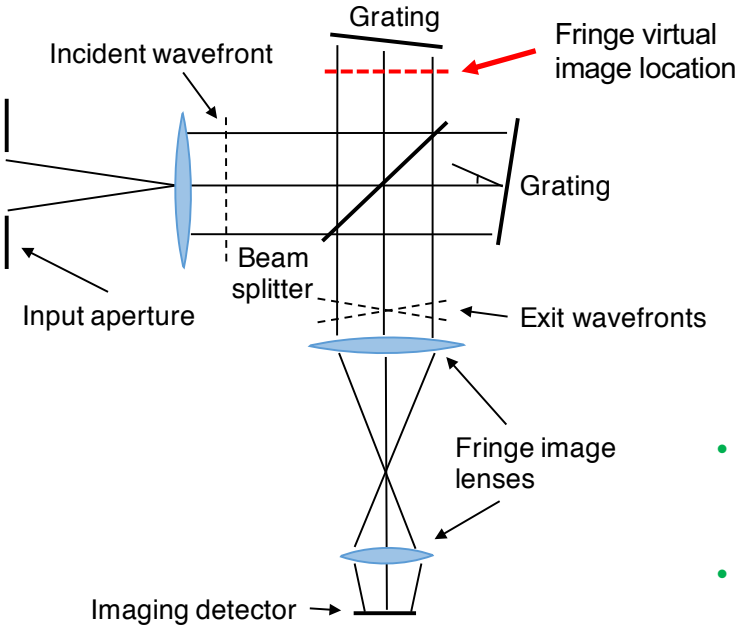

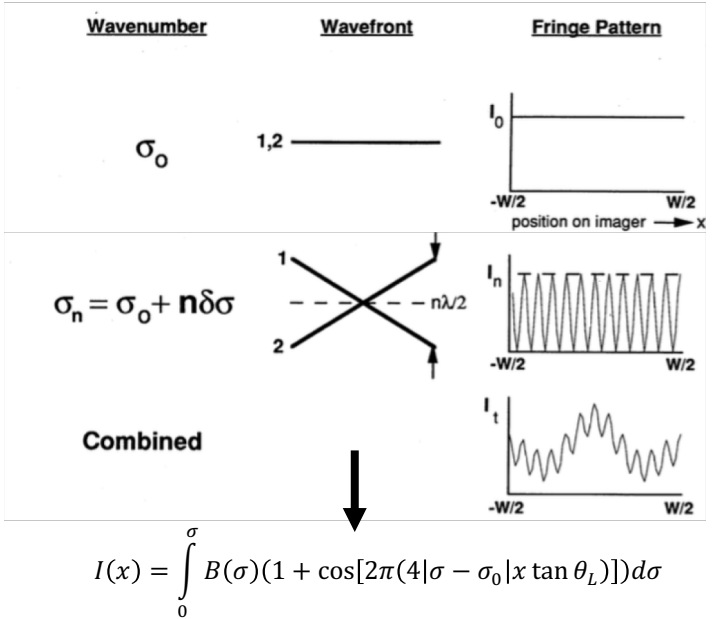

$$I(x) = \int_0^\sigma B(\sigma)(1 + \cos[2\pi(4|\sigma - \sigma_0|x \tan\theta_L)])d\sigma$$

- **Interferometer class spectral resolution and throughput without moving parts**
- **$R \sim 10^4$ and $U = 0.016$ cm²sr can be readily obtained with relatively small optics compared to slit systems**

J. Harlander, R. J. Reynolds, and F. L. Roesler., ApJ, **396,** 1992.

Spectrometer Design Points for Field Test at DIII-D

- SHS prototype ("Phase I") designed, built, and evaluated at UW-Madison
  - System design for flexibility, built with "stock" optics
- Field tests at DIII-D:
  - Photon flux adequate for ~1% photon statistics turbulence measurement
  - Evaluation of vibrational environment → requires multi-level isolation strategy for next stage SHS
  - Experience with SHS data analysis
- Next stage SHS for turbulence measurement being built
  - ~500 kHz detector system
  - Fast, robust, analysis algorithm for $\tilde{\mathbf{E}}$ extraction

$\tilde{\mathbf{E}}$ diagnostic system parameters:

Parameter	Units	Value
Design spectral resolution @ 656 nm	nm (cm^{-1})	0.086(2)
Max throughput	mm^2 sr	4.8
Grating width	cm	7.62
Grating groove density	mm^{-1}	50
Sampling speed	kHz	430-700
Image size	mm	2x2
f/# at detector		1
D_α filter transmission	%	>95
D_α filter 90-10% cutoff & uniformity	nm	0.2
Fringe imaging system magnification		0.033

First Plasma Light Through Prototype SHS

- Several interferometer components tested at D3D before LTO3
- Prototype SHS and survey spectrometer (1/2 m Princeton Instruments, 100 μm slit) beam emission spectrums are comparable
  - Input: Two radially adjacent channels from BES fiber array
  - Linear polarizer removes σ components
- $R \cdot U \equiv \frac{\lambda}{\delta\lambda} \cdot \frac{\pi A_s}{4(f/\#)^2}$ product:
  - 1/2 m Czerny-Turner ($\delta\lambda$=0.05 nm) = 0.73
  - SHS ($\delta\lambda$= 0.13 nm) = 128

SHS output produced by tokamak light with linear polarizer installed at machine:

Raw Fizaeu fringes:

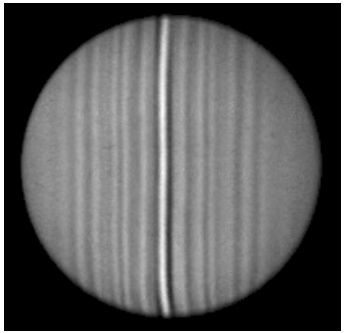

Total photon flux through SHS: ~5×10^9 sec^{-1}

SHS Instrument Function:

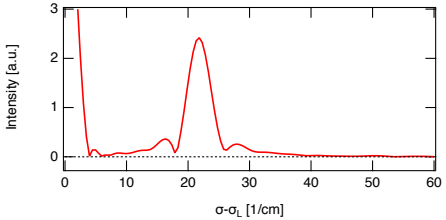

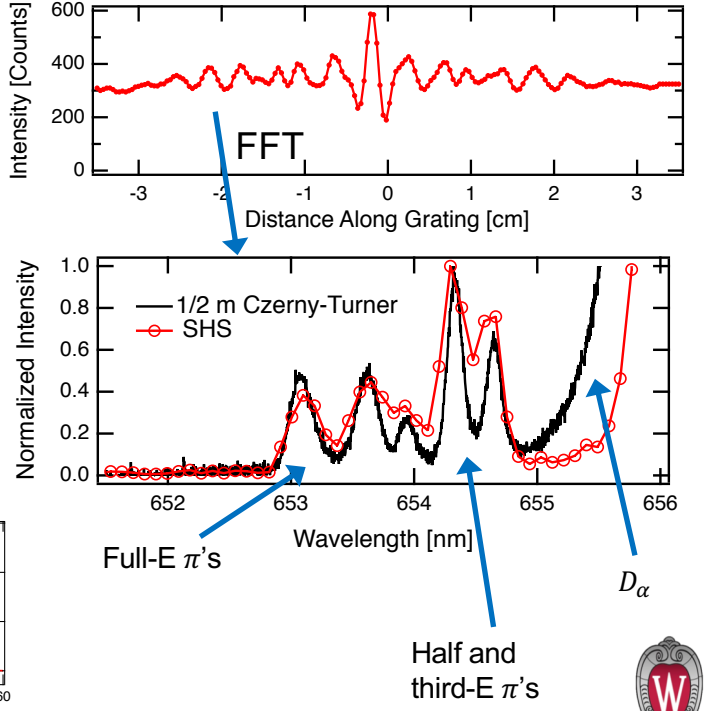

Burke M.G., *et al.*, Rev. Sci. Inst., (2018)

Phase I deployed to D3D for Evaluation in Tokamak Environment

Prototype SHS in D3D BES Diagnostic Lab

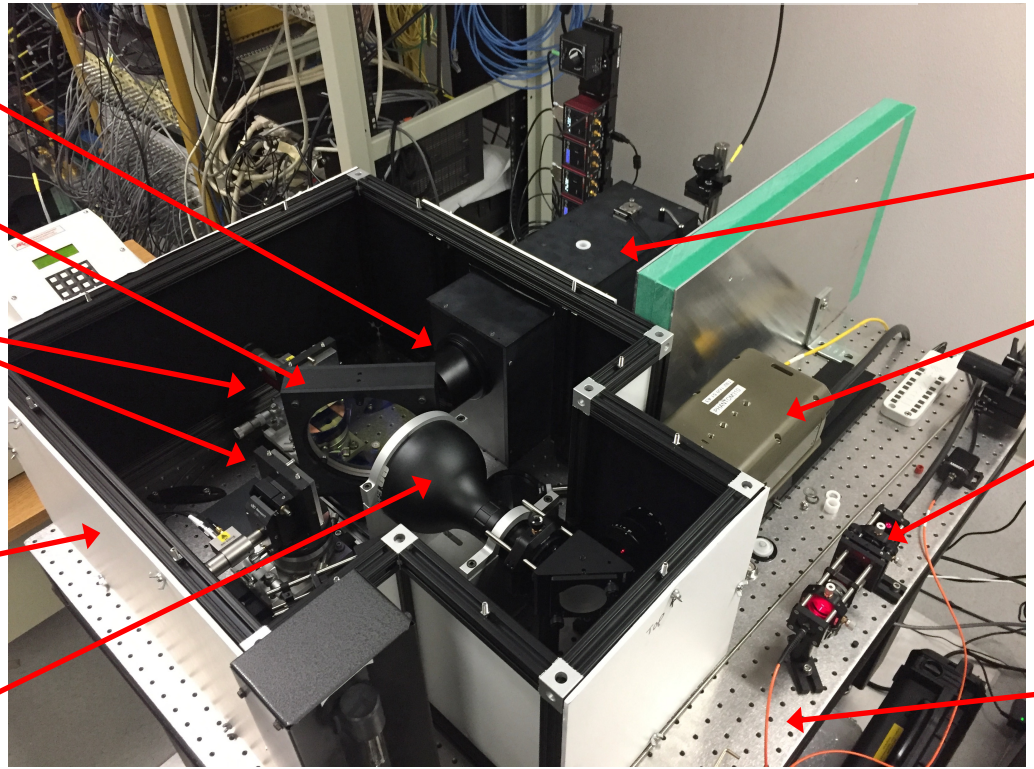

Design Modification and Upgrades for Next Stage SHS

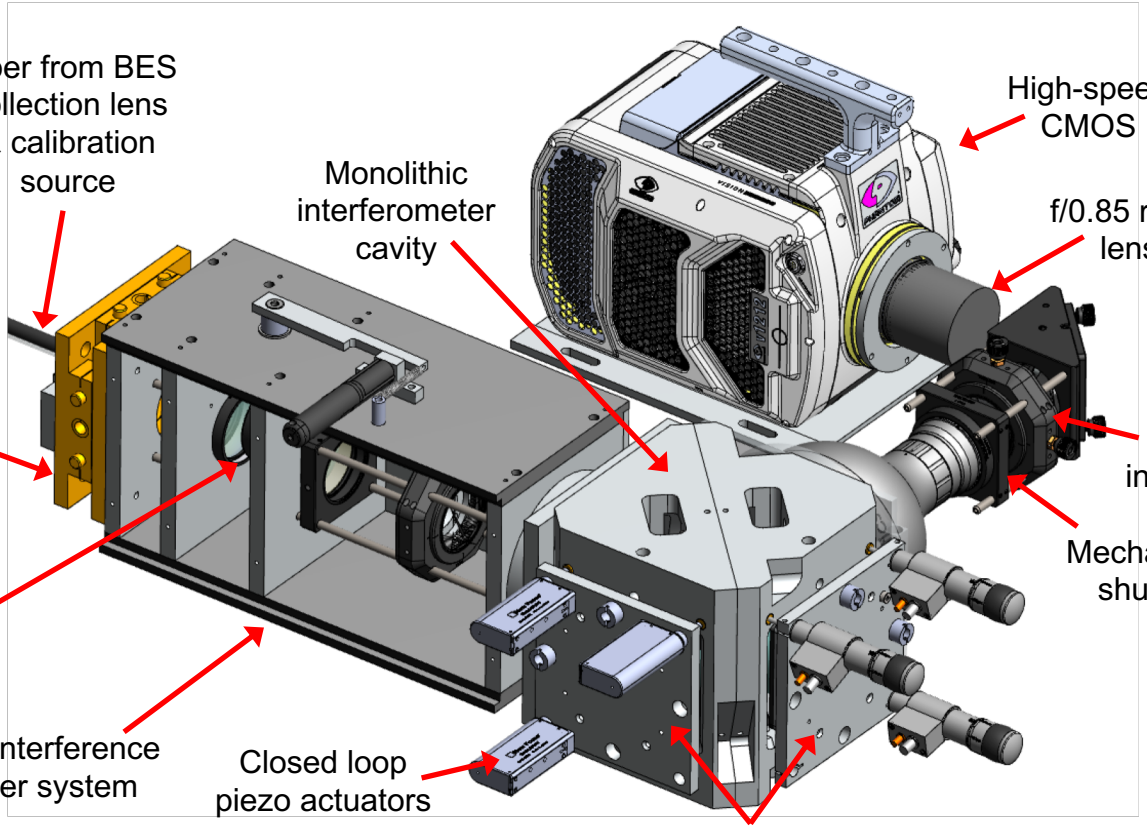

Diagnostic Layout

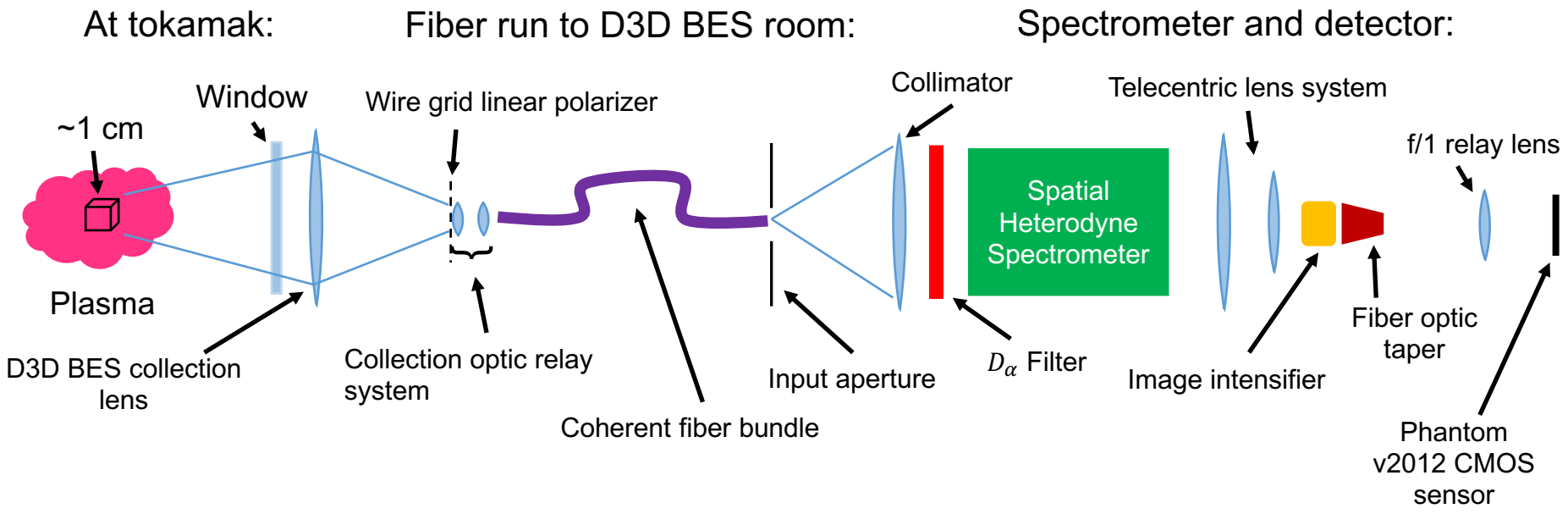

$\tilde{E}$ Extraction Algorithm

$\tilde{E}$ Extraction with Weighted Linear Least Squares Algorithm

- **Motivation:** need fast & robust algorithm with good noise performance to extract $\tilde{E}(t)$ from ~20 gigabyte/shot photon noise limited dataset
- Stark SHS interferogram nonlinear function, but highly symmetric → linearize → best-fit $\tilde{\mathbf{E}}$ extracted from interferogram via multiple linear regression analysis method (least-squares fit)

$$I(\sigma, x) = \int S(\sigma)\,(1 + \cos[8\pi x \tan\theta_L\,((\sigma_{D0} \pm \Delta\sigma(\mathbf{E_t})) - \sigma_L)]\,d\sigma$$

$$I_\pi(x) = S_0 \sum_{n=2}^{4} a_n\left(2 + 2e^{-\pi(4x\tan\theta_L w)^2}\cos(\phi_{avg})\cos(\phi_{diff})\right)$$

$$\phi_{avg} = 8\pi x \tan\theta_L\,(\sigma_{D0} - \sigma_L), \qquad \phi_{diff} = 8\pi x \tan\theta_L\, n\delta(|\mathbf{E_{MSE}}| + |\mathbf{E_p} + \tilde{\mathbf{E}}|)$$

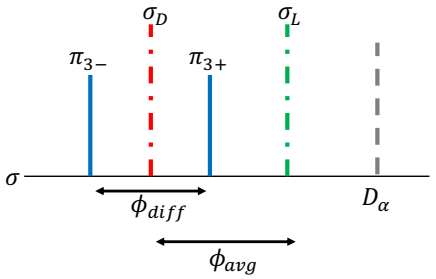

- $\tilde{\mathbf{E}}$ results in very small changes in <u>only</u> ϕ_{diff}
- Linearized interferogram: full-energy only, six π-components with peak broadening:

$$I(x) = S_0\left[2(a_2 + a_3 + a_4) + 2e^{-\pi(4x\tan\theta_L w)^2} a_n \cos(Ax(\sigma_{D0} - \sigma_L))(\cos(Axn\delta|\boldsymbol{E_{MSE}}|) + \cdots)\right]$$
$$-|\tilde{\boldsymbol{E}} + \boldsymbol{E_p}|S_0\delta\left[2e^{-\pi(4x\tan\theta_L w)^2} A a_n x n\ \cos(Ax(\sigma_{D0} - \sigma_L))(\sin(Axn\delta|\boldsymbol{E_{MSE}}|) + \cdots)\right]$$

- Linear in coefficients $S_0 = c_1$ and $|\tilde{\mathbf{E}} + \mathbf{E_p}|S_0\delta = c_2$ → interferogram in form $y(x_i) = \sum_{k=1}^{m} c_k f_k(x_i)$

$\tilde{E}$ Extraction Algorithm works up to ~100 kV/m

- Fit interferogram data via fast matrix inversion with weights

$$\mathbf{c} = \boldsymbol{\beta}\boldsymbol{\alpha}^{-1} \quad \boldsymbol{\beta}_k = \sum \frac{1}{\sigma_i^2} y_i f_k(x_i) \quad \boldsymbol{\alpha}_{lk} = \sum \frac{1}{\sigma_i^2} f_l(x_i) f_k(x_i)$$

- Several assumed constants in fitting algorithm:
  - V_{beam} (beam voltage): unknown, can be characterized, high voltage beam diagnostic suggests $\Delta_{V_{beam}}$~ 200 Vrms
  - Stark component relative intensity: weak dependence on n_e (Marchuk *et al.,* 2010)
  - Component spectral width, w: beam divergence, source temperature, geometric broadening → Needs to be characterized via beam-into-gas studies
- Fit algorithm linear with ≲1% error out to $\tilde{E} + E_p$ =100 kV/m over range of beam energies

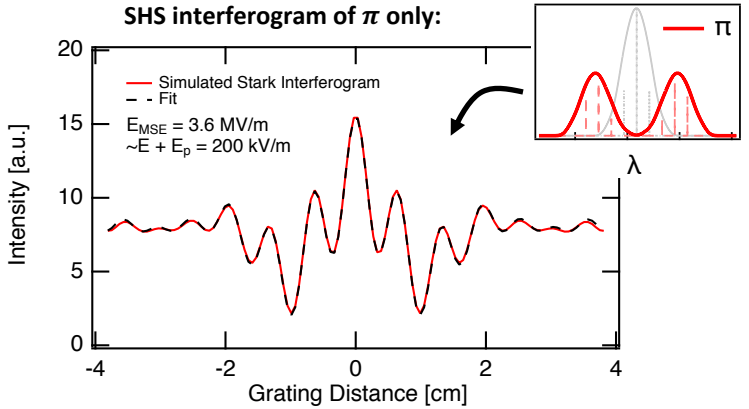

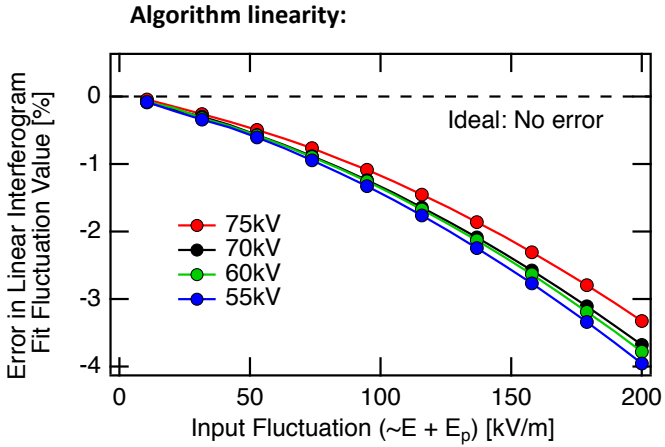

Noise in Fitted $\tilde{\mathbf{E}}$ is Proportional to Photon Noise

- **Algorithm noise evaluation:** Scaling of $\varepsilon_{\tilde{\sigma}}/w$ vs relative photon noise and absolute uncertainty of $\tilde{\sigma}$ [cm^{-1}] ($\tilde{\mathbf{E}}$ [kV/m])
- Measured total beam emission spectrum SNR~100 at 500 kHz using SHS prototype at D3D
- Monte-Carlo studies evaluated $\tilde{\mathbf{E}}$ sensitivity with photon/amplifier noise, spectrometer parameters, Stark spectrum model
  - 1000 interferograms generated with Poisson noise applied given SNR, no perturbation ($\tilde{\mathbf{E}} = 0$)
  - $\varepsilon_{\tilde{\sigma}}(\tilde{\mathbf{E}})$, standard deviation of fitted spectral fluctuation value
  - w, standard deviation of width of individual π components
- Uncertainty in fitted spectral fluctuation ($\tilde{\mathbf{E}}$) scales linearly with relative photon noise

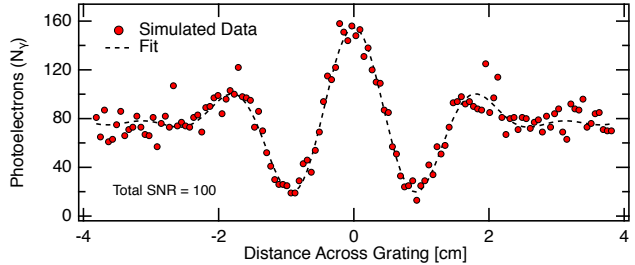

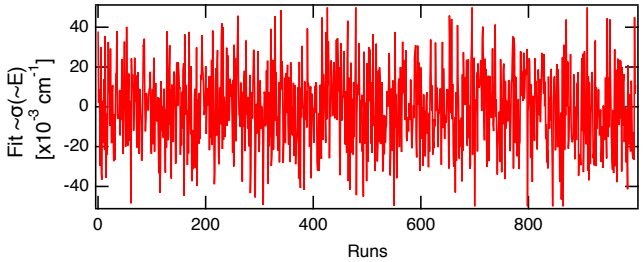

Example interferogram noise scaling:

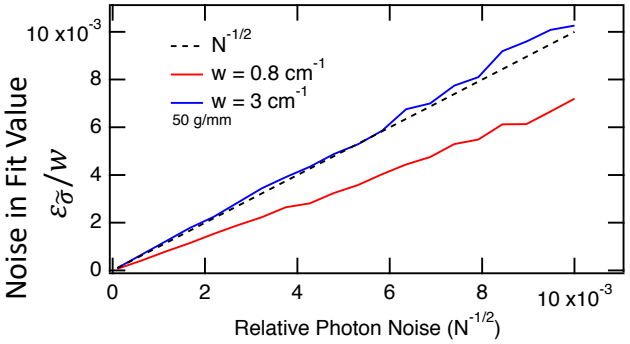

Monte-Carlo Studies Used to Determine Spectrometer Parameters

- Lower fluctuating wavenumber uncertainty ($\varepsilon_{\tilde{\sigma}}$) is better
- Optimal groove density (i.e. SHS resolution) that maximizes sensitivity to $\tilde{\mathbf{E}}$ is ~25 g/mm
- Spectral width of individual Stark components reduces sensitivity
- Number of detector pixels required depends on the complexity of the interferogram → controllable by Littrow wavenumber
  - ~64 pixels adequate to fully resolve fluctuations in complex interferogram
  - Sub sampling with reduced pixel number must be matched to Littrow wavenumber configuration
  - Likely want more pixels than 64 so facilitate distortion correction of 2D interferogram

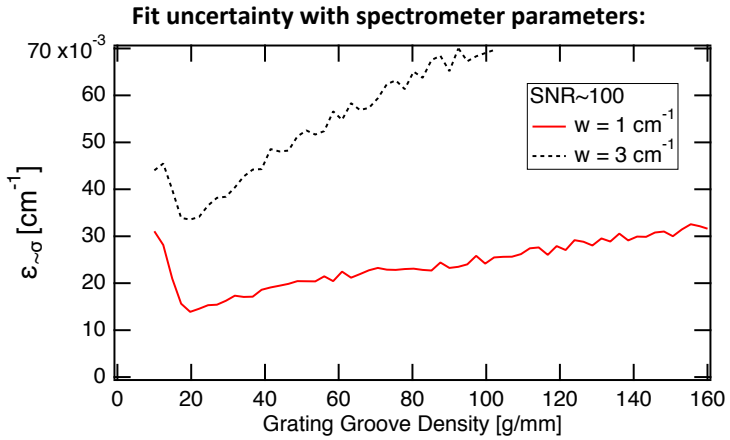

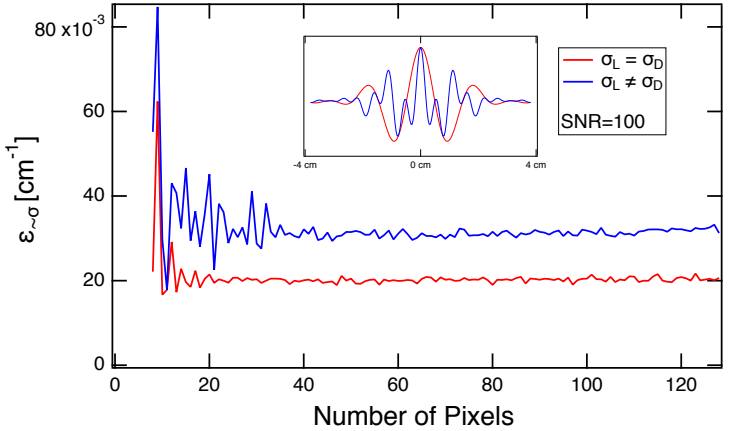

Littrow wavenumber Placement Can Maximize SNR

- Stark $\pm\pi$-components are symmetric about Doppler shift wavenumber (σ_D)
- Placing $\sigma_L = \sigma_D$ gives lowest $\varepsilon_{\tilde{\sigma}}$
- Placing $\sigma_L = \sigma_D$ effectively doubles the SNR in the spectral domain (see FFT of interferogram)
- Maintaining the interferometer at $\sigma_L = \sigma_D$ could be challenging
  - Mechanical vibrations and thermal swings must be counteracted
  - Requires *in-situ* calibration/monitoring of σ_L
- Wavefront errors maximized here, 2D detector allows for phase correction data processing

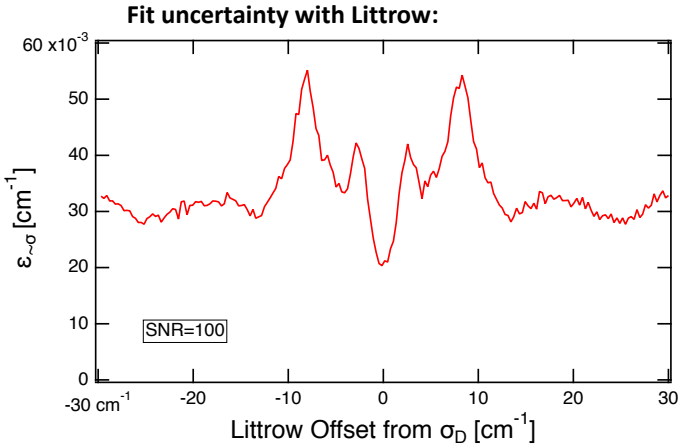

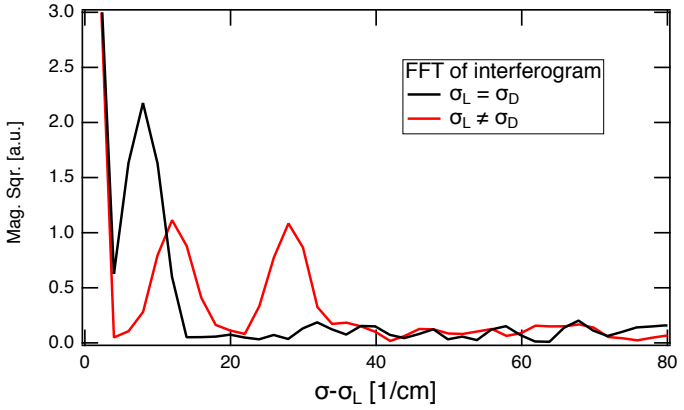

SHS has Built in Correlation Detection Capabilities

- Symmetry of SHS interferogram allows for ~10x reduction of photon noise floor via cross correlation of the two sides of the interferogram
  - SHS optical path different (OPD) in terms of $\delta\sigma = |\sigma - \sigma_L|$
  - Splitting the interferogram at zero-path-length-difference point provides two measurements of same quantity ($\tilde{\mathbf{E}}$) → cross correlation suppresses incoherent photon noise present in both measurements
  - Can be done with single spatial channel
- Long time records required to pull ~E from background
  - Example plot: 10 kHz BW, 1 second data record with 1 MHz sampling
- Combination of techniques allows for fluctuations of order 1 kV/m to be measured from signal with ~1% photon noise
  - D3D $\tilde{\mathbf{E}}$ estimated to be ~3 kV/m in core region, larger at edge

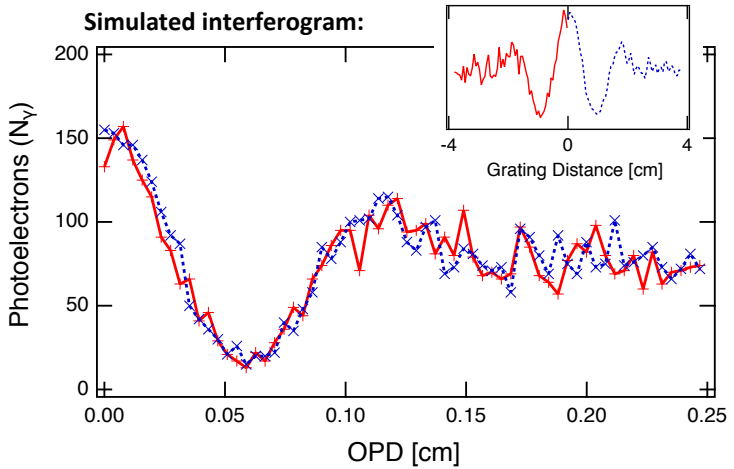

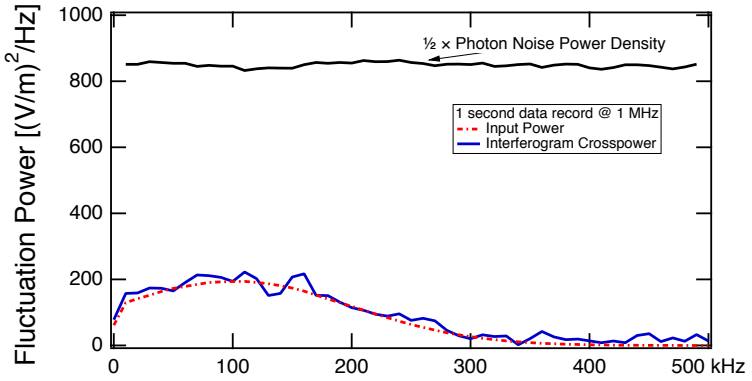

Geometric Doppler Shift Correction via Offset Aperture in SHS

- Similar Doppler shift correction utilized in planetary wind Fabry-Perot spectroscopy techniques*
- At spectrometer, window image rotated 90° so that $\Delta\sigma_D$ is perpendicular to dispersion plane ($\Delta\sigma_D(\alpha)$, where α is angle off dispersion plane)
- SHS interferogram equation phase can be rederived to include small aperture offset angle α_0, $\alpha = \alpha_0 \pm \phi$ (ϕ is spectrometer field of view) :

$$\sigma d \cos\alpha\,(\sin\theta_{in} + \sin\theta_{out}) = m$$

$$\Phi(x) = 2\pi\left(4x\tan\theta_L\left[-\delta\sigma_D + \frac{\sigma}{2}(\beta^2 + \phi^2 + 2\phi\alpha_0 + \alpha_0^2)\right]\right)$$

For Doppler compensation: $-\delta\sigma_D + \sigma\phi\alpha_0 = 0$

- For $\delta\lambda_D$~0.4 nm, $\phi_{max} = \sqrt{8/R}$~16 mrad → ~30 mrad

Doppler compensation concepts in SHS:

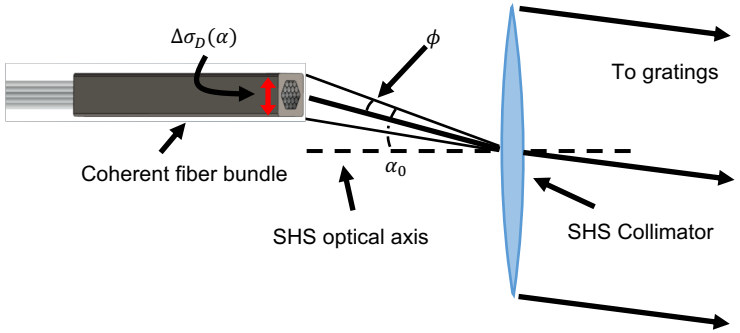

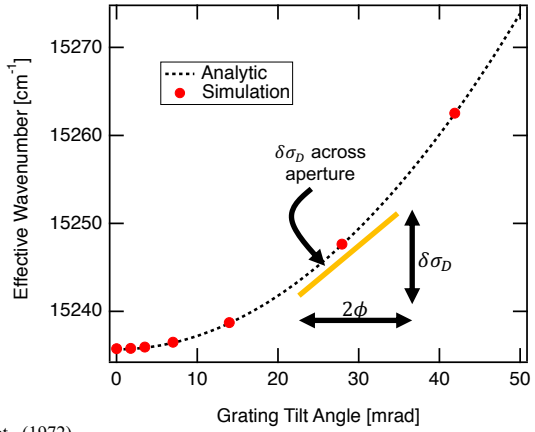

Ray trace simulation:

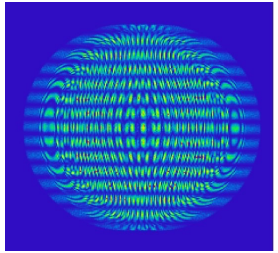

α_0= 26 mrad
$\delta\sigma_D$ = 9 cm^{-1}
ϕ = 7 mrad

*Trauger & Roesler, Appl. Opt., (1972)

Geometric Broadening Compensation: Collection Lens Relay System to SHS

- Small relay lens system designed to place image of collection optic at fiber bundle with minimal loss of light and plasma spatial resolution
- Lenses create ~3mm spot size, convert from f/3 to f/2
- New fiber bundle run cuts collection lens into 5 regions

Ray trace: reimaging of D3D BES collection lens:

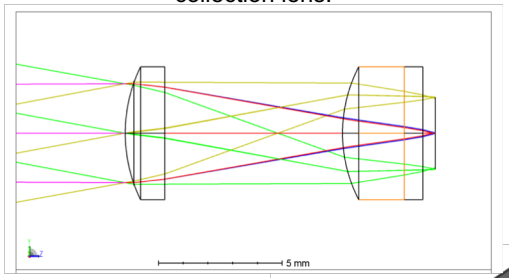

Backlighting bundle w/ lenses:

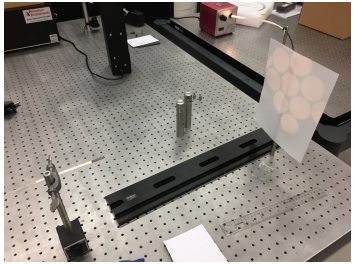

Relay lens system fits within existing BES infrastructure:

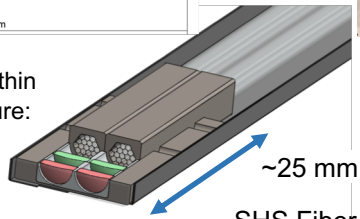

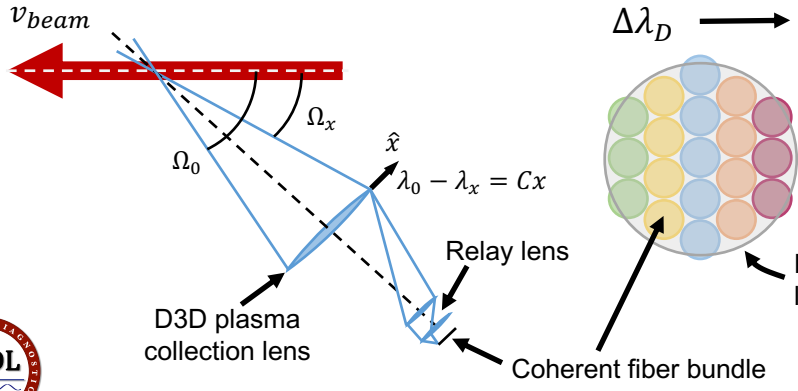

SHS Fiber with relay:

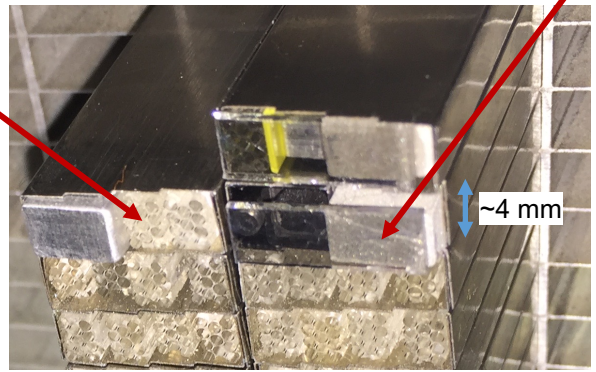

Algorithm in Place to Extract $\tilde{E}$

- Least squares fit algorithm to Stark SHS interferogram is fast, robust (small-to-zero failure)
- Least squares algorithm performs similarly to Levenberg-Marquardt nonlinear fit algorithm
- Overall spectral width, w, has strong effect on $\varepsilon_{\tilde{E}}$
- Stark spectral modeling indicates w can be reduced ~2.5x

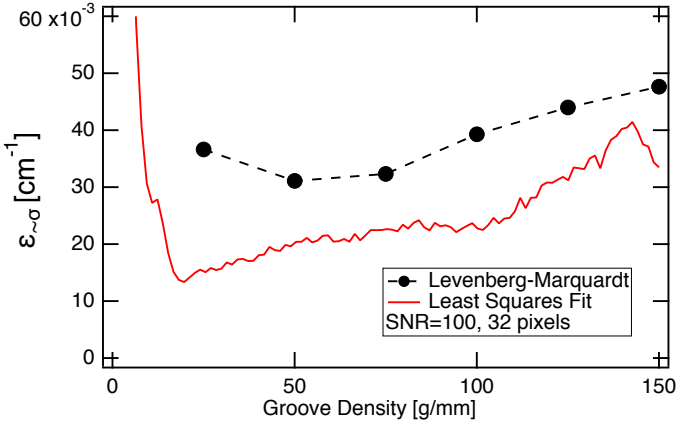

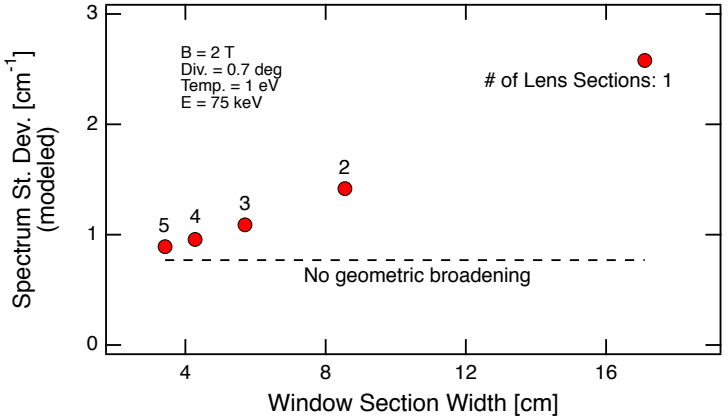

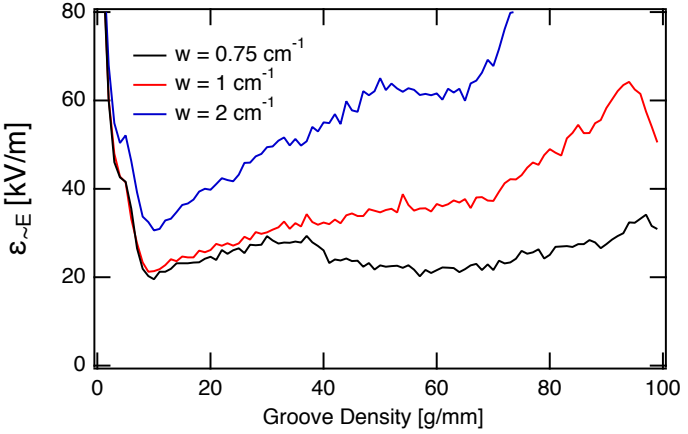

SHS Detector Requires High Internal Gain and Low Additive Noise

- SHS output requires high-speed 2D imaging detector
  - SHS produces ~75mm diameter interferogram image, minified ~36X at detector
  - Detector sampling rate ≳400 kHz covers most commonly observed low-k broadband turbulence and low frequency coherent modes ($\tilde{n}$: GAMs, $\tilde{B}$: EHO & RMP)
- Spectral resolving beam emission results in ~1% total flux in given bin
  - Flux per spectral bin well below high-performance photodiode amplifiers
- 3rd generation photocathodes and production techniques allow photo-multiplying devices (microchannel plates, hybrid SI-diode tubes) to be comparable to high-QE devices (APDs)
  - Avalanche Photodiode: QE~80%, Gain~250, Excess noise~2.5, Net QE~32%, $
  - Hybrid Si-diode tube: QE~40%, Gain~10^5, Excess noise~1, Net QE~40%, $$$$
  - GaAs photocathode & microchannel plate: QE~35%, Gain~10^4, Excess noise~1.1, Net QE~32%, $

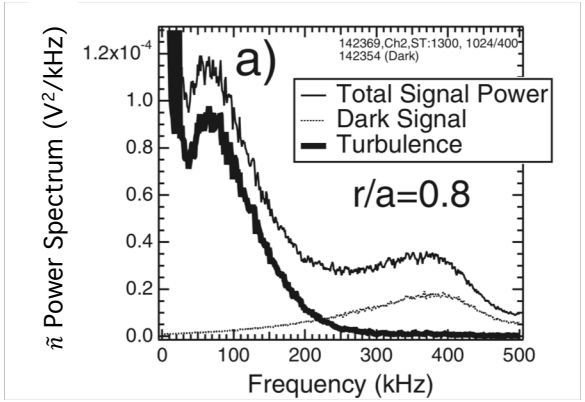

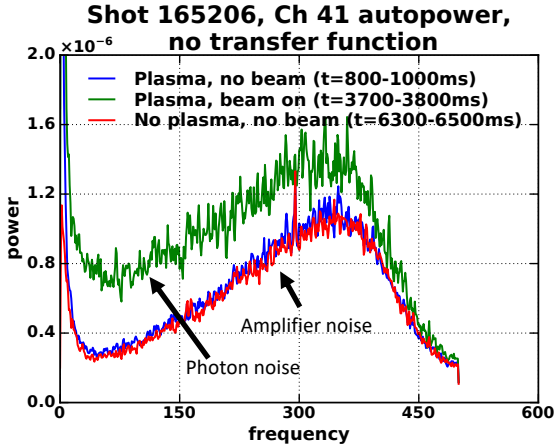

G. Mckee, *et al.*, Rev. Sci. Inst., (2010)

Intensified CMOS to be Detector System For Diagnostic Validation

- Easier coupling to SHS output image (no fiber bundle coupling or reimaging losses)
- Equivalent QE to APD with more gain
- Excess noise in image intensifiers driven by MCP open-area ratio (ϑ) and noise in first stage gain (g_p)

$$\varepsilon_{out}^2 = F\varepsilon_{in}^2, \qquad F \approx \frac{1}{\vartheta}\left[1 + \frac{1}{g_p}\right]$$

  - g_p typically 5-10 due to MCP entrance coating
- 98% collection efficiency MCP and coating design push excess noise (F) to ~1.1
- Modest gain needed to become photon noise dominated when binning over M pixels

$$\frac{\varepsilon_S^2}{S^2} = \frac{1}{N_T}\left[1 + \frac{1}{g_p - 1}\right] + \frac{1}{M(g_p - 1)} + \frac{M\varepsilon_R^2}{N_T^2 \bar{G}^2}$$

2D Interferogram with noise:

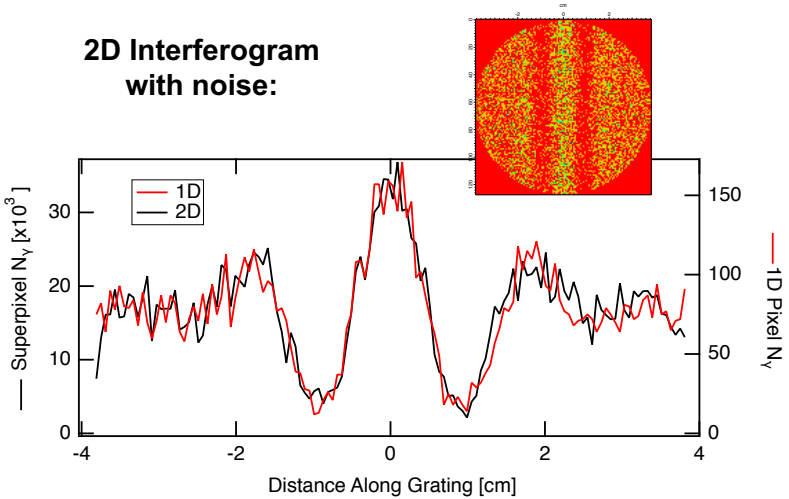

Fit wavenumber uncertainty ($\varepsilon_{\bar{\sigma}}$) with 2D detector noise:

Interferogram	Gain	Excess Noise (F)	Readout Noise (ε_R)	$\varepsilon_{\bar{\sigma}}$ $[cm^{-1}]$
1D	1	1	0	0.0187
2D	250	1	27 phe-	0.0199
2D	250	1.2	27 phe-	0.0256

*1% photon noise, M=128

Experience with Intensified CMOS Indicates Photon Noise Limited Performance

Phantom v310 and Proxitronix UV intensifier:

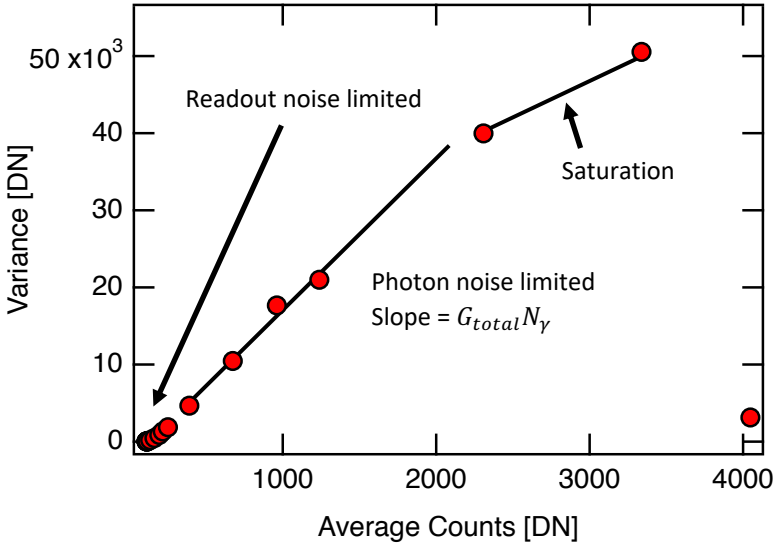

G_{total} includes camera gain, sensor QE, total intensifier gain, coupling optic efficiency,

SHS Detector Parameters: Phantom v2012 & Photonis GaAs Image Intensifier

Parameter	Units	Value
Max Spectral Bins	Pixels	128
Sample Rate	kHz	670 (128x80 pixels) 430 (128x128 pixels)
MCP Open-Area-Ratio	%	>95
MCP Saturation Current	μA	18-40
Photocathode QE	%	35
Phosphor 90-10% Decay Time	ns	~300
Max Gain	W/W	5000
Readout Noise	photoelectron	27
Dynamic Range	dB	57
Pixel Size	um	28

Summary

- Analysis technique based on least-squares linear regression algorithm extracts $\tilde{\mathbf{E}}$ from ~20 Gb/shot data set
  - Algorithm $\tilde{\mathbf{E}}$ fit value scales linearly with relative photon noise
  - Monte Carlo studies inform SHS design and maximize sensitivity to $\tilde{\mathbf{E}}$
  - Inherent correlational detection technique and ~1 second time records give sensitivity to $\tilde{\mathbf{E}}$ on the order of 2 kV/m
- Intensified CMOS detector designed/being built for diagnostic technique validation
  - Combines Phantom v2012 with Photonis high collection efficiency MCP GaAs image intensifier
  - Detector designed for high speed (~500 kHz), high internal gain (10^4) with low excess noise (F~1.1)
- Final testing at UW, deployment to D3D in mid-2019

Work supported by US DOE grant DE-FG02-89ER53296.

Layout Slide (Include for Posters)

12:1 scale Panel size: 8’ x 4’

Title Strip

Introduction	Diag. Requirements	Predictive Modeling	Detector Development	
Understanding Turbulence in Tokamaks is a Fundamental Challenge for Fusion Energy	$\tilde{E}/\vec{E}_{MSE}$ in Fusion Grade Plasmas is ~10^{-3}	Linearized Interferogram Derivation		
Motional Stark Effect Field Used as Carrier Signal for $\tilde{E}$ and $\tilde{B}$	How SHS works			

Summary: Validation and Field Tests of Spatial Heterodyne Spectrometer for $\tilde{E}$ Measurement

- First field tests of prototype SHS for $\Delta\tilde{\lambda}_\pi \propto \tilde{E}$ measurement completed
  - Spectrometer validated at $\lambda\delta \approx 0.16$ nm and $U \approx 0.03$ cm^{2}sr
  - Signal level gives ~1% photon statistics, adequate for turbulence measurements (room for improvement with custom gratings & new detector system)
  - Produced BES spectrum with SHS, observed rapid changes in fringe pattern corresponding with beam modulations
- Development for Turbulence Measurements on DIII-D: Construct & Deploy “Phase 2”
  - Fabricate final detector system (either intensified phantom or multianode MCP: ~1 MHz sampling, low readout noise)
  - Address lab vibrations with monolithic low thermal expansion grating-beam splitter mount design, or discuss moving spectrometer
  - Continued development of high speed fringe data analysis algorithms: focus on sensitivity with noise
  - Off-line validation of geometric Doppler broadening compensation technique for SHS
  - Integrating multiple spatial points into single spectrometer

Monte-Carlo Studies of spectrometer Predict $\tilde{E}$ Sensitivity

- Expect uncertainty in LSF spectral fluctuation to scale similarly to gaussian fit location (μ) uncertainty in spectral domain, $\varepsilon_\mu \rightarrow \frac{\mathrm{Var}[\varepsilon_\mu]}{w^2} = \frac{1}{N_\gamma}$
- LSF $\varepsilon_{\tilde{\sigma}}/w$ deviates from expected $N_\gamma^{-1/2}$ scaling over range of spectrometer parameters
  - Slope $< 1 \rightarrow \varepsilon_{\tilde{\sigma}}$
- This analysis is ongoing → general trends